Phase-locked patterns and amplitude death in a ring of delay-coupled limit cycle oscillators

Ramana Dodla,* Abhijit Sen,† and George L. Johnston‡
Institute for Plasma Research, Bhat, Gandhinagar 382428, India
(Received 19 November 2003; published 24 May 2004)

We study the existence and stability of phase-locked patterns and amplitude death states in a closed chain of delay coupled identical limit cycle oscillators that are near a supercritical Hopf bifurcation. The coupling is limited to nearest neighbors and is linear. We analyze a model set of discrete dynamical equations using the method of plane waves. The resultant dispersion relation, which is valid for any arbitrary number of oscillators, displays important differences from similar relations obtained from continuum models. We discuss the general characteristics of the equilibrium states including their dependencies on various system parameters. We next carry out a detailed linear stability investigation of these states in order to delineate their actual existence regions and to determine their parametric dependence on time delay. Time delay is found to expand the range of possible phase-locked patterns and to contribute favorably toward their stability. The amplitude death state is studied in the parameter space of time delay and coupling strength. It is shown that death island regions can exist for any number of oscillators N in the presence of finite time delay. A particularly interesting result is that the size of an island is independent of N when N is even but is a decreasing function of N when N is odd.

DOI: 10.1103/PhysRevE.69.056217 PACS number(s): 05.45.Xt, 87.10.+e, 02.30.Ks

I. INTRODUCTION

The emergence of self-organized patterns is a common feature of nonequilibrium systems undergoing phase transitions. Examples of such patterns abound in nature ranging from intricate mosaic designs on a butterfly wing, vortex swirls in a turbulent stream to synchronous flashing of fireflies [1]. The study of pattern formation and self-synchronization using simple mathematical models consisting of coupled differential equations has therefore been an active area of research spanning many scientific disciplines. For example such models have been employed to examine the collective output of arrays of lasers [2,3], coupled magnetrons [4], Josephson junctions [5], coupled chemical reactors [6,7] and electronic circuits [8]. Rings of oscillators have also been useful for modeling biological oscillations [9,10] and simulation of phase relations between various animal gaits [11]. These simple discrete models (usually composed of coupled limit cycle oscillators) are amenable to some straightforward analysis and also direct numerical solutions particularly when the number of oscillators is small. When the number of oscillators becomes very large it is often convenient to go over to the continuum limit of infinite oscillators and model the system with a partial differential equation. Examples of the latter are reaction-diffusion-type mathematical equations, such as the time-dependent complex Ginzburg-Landau equation (CGLE), which have been widely used to simulate the dynamics of pattern formation in fluids and other continuum systems [12]. One of the most popular of the discrete models is the "phase only model" that arose from the pioneering contributions of Winfree [9] and Kuramoto and co-workers [13,14]. This model is valid as long as the coupling between the oscillators is assumed to be weak so that amplitude variations can be neglected. When the weak coupling approximation is relaxed and amplitude variations are retained the system is found to admit new collective states such as the amplitude death state [15–17], chaos, and multirhythmicity [18–21]. This strong coupling model has received a great deal of attention in recent times [11,17,22–24]. The importance of time delay in coupled oscillator systems and its effect on their collective dynamics has been recognized for a long time. In particular, there have been a large number of studies devoted to the study of time delay coupled phase-only models [25–34]. More recently, the strong coupling model has also been generalized to include propagation time delays [35–38]. A number of interesting results regarding collective oscillations have emerged from this generalized time delayed model, some of which have been experimentally verified [39–41].

Our present work is devoted to further investigations and understanding of the generalized time delay coupled model. Most of the past investigations on this model have been restricted to collective states emerging from *global coupling* among the oscillators, also known as the mean field approximation. We have chosen to study here the equilibrium and stability of collective modes emerging from a time delay coupled system of identical oscillators in which the coupling is *local and restricted to nearest neighbors*. The choice of this model is motivated by several considerations. From a basic studies point of view the model offers us an opportunity to compare and contrast the properties of the collective states of the local coupling geometry to that of the globally coupled states. The model further permits a parametric study of the influence of the number of oscillators N on the stability and existence properties of the equilibrium states. In the limit of large N the model also has close resemblance to the

*Present address: Center for Neural Science, New York University, New York, NY 10003. Electronic address: ramana.dodla@nyu.edu. (The author's name appeared earlier as D. V. Ramana Reddy.)
†Electronic address: abhijit@ipr.res.in
‡Present address: EduTron Corp., 5 Cox Road, Winchester, MA 01890. Electronic address: glj@rcn.com

continuum CGLE and it is of interest to delineate the important differences in the collective properties of the two systems. From a practical point of view our model has great relevance for many physical systems including coupled magnetrons, study of collective phenomena in excitable media, coupled laser systems, and small-world networks. For example, an interesting study on the role of the geometry of the coupled magnetrons on their rate of phase locking was made by Benford *et al.* [4] who experimentally demonstrated production of higher microwave power at gigawatt levels through phase locking. Our analysis of nearest neighbor coupled oscillator array could provide important clues on not only the effect of circular geometry but also on the effects of time delay in such a geometry. A ring of coupled oscillators is also commonly encountered in a variety of biological clocks [9]. For simplicity of analysis most mathematical studies of these rings have been confined to an examination of their phase evolutions. Our model analysis can provide an extended understanding of these biological clocks with the inclusion of time delays and amplitude effects. Another interesting and more recent potential application of our work is in the rapidly developing area of small-world networks where the simplest studied configuration is often a ring of oscillators with nearest neighbor connections dominating [42]. A recent study has explored the role of time delays in a ring of connected oscillators with a special focus on small-world networks [34]. We believe that our present study of the ring configuration could help provide further insights in this direction with the incorporation of amplitude effects.

The existence of equilibrium states of locally coupled oscillator systems has been studied in the past using group theoretic methods [43,44]. We use a plane wave method and investigate both the existence and stability regions of the equilibrium states of the coupled system. We derive a general dispersion relation that can be used to determine the equilibrium states of any number of coupled oscillators. The method is further extended to a linear stability analysis of these equilibrium states. Using this technique we delineate the existence regions of the various equilibrium phase-locked patterns of the coupled system. In the limit of small N and in the absence of time delay our results agree with past findings, but we also find new equilibrium states that have not been noticed before. With time delay the existence regions change in a significant manner and in some of the regimes we observe multirhythmicity. Finally, we also examine the nature of the death state in our system in the presence of time delay. Although time delay induced death state in locally coupled identical oscillators has been numerically observed in one of our past studies [35] there has been no systematic analytic investigation of this phenomenon. We carry out such an analysis here and delineate the existence of the death region as a function of the time delay and coupling strength parameters. Our analysis yields an interesting result in that the size of the *death island* is found to be independent of N (the number of oscillators) when N is even but is a decreasing function of N when N is odd.

The paper is organized as follows. In the following section we present the model equations and briefly discuss their similarities and differences with the continuum model CGL equation. Using the plane wave method we next derive the dispersion relation in Sec. III and proceed to use it to delineate the possible existence regions of the phase-locked patterns both in the presence and absence of time delay. Section IV is devoted to a linear stability analysis of these states in order to identify their actual existence domain. In Sec. V we briefly look at the stability of the origin, which is the existence domain of the death state, as a function of the time delay parameter and the coupling strength. Our results are summarized and their implications discussed in the concluding Sec. VI.

II. MODEL EQUATIONS

We consider a one-dimensional closed chain of delay coupled identical limit cycle oscillators that are close to a supercritical Hopf bifurcation. Assuming the coupling to be linear and of the nearest neighbor kind, we can write down the following set of model equations to describe the time evolution of the oscillator states:

$$\frac{\partial \psi_j}{\partial t} = (1 + i\omega_0 - |\psi_j|^2)\psi_j + K[\psi_{j+1}(t-\tau) - \psi_j(t)] + K[\psi_{j-1}(t-\tau) - \psi_j(t)], \quad (1)$$

$j=1,\ldots,N$, where $\psi_j(=X_j+iY_j)$ is the complex amplitude of the jth oscillator, $K>0$ is the coupling strength, $\tau \geqslant 0$ is a fixed time delay, and ω_0 is the natural frequency of the uncoupled oscillators. The basic nonlinear oscillator we have chosen here is simply the normal form of the supercritical Hopf bifurcation equation truncated to the third order. It is also known as the Stuart-Landau oscillator and has been extensively used in the past as a model equation for studying nonlinear phenomena in fluids, lasers, and Josephson junctions. For example, in the absence of time delay ($\tau=0$), the above set of equations (1) have been used to study the coupled wakes arising from a flow behind an array of equally spaced parallel cylinders [45]. Another interesting connection to past work is the continuum limit for $\tau=0$, where one can introduce a lattice spacing a, set $\psi_j=\psi(ja)$ in Eq. (1), rescale K as K/a^2, and then let $a\to 0$ with $ja\to x$. This reduces Eq. (1) for $\tau=0$ to the well-known complex Ginzburg-Landau equation

$$\frac{\partial \psi(x,t)}{\partial t} = (1 + i\omega_0 - |\psi(x,t)|^2)\psi(x,t) + K\frac{\partial \psi^2(x,t)}{\partial x^2}. \quad (2)$$

The CGLE has been extensively investigated in the past for its rich equilibrium states and for their applications to a variety of physical situations [46,47]. In the presence of time delay it is not meaningful to take the continuum limit since $a\to 0$ would also make the propagation time tend to zero. One can instead take the so-called thermodynamic limit by letting $N\to\infty$ and the chain length $L\to\infty$, while keeping $a=L/N$ fixed. In such a limit the time delay parameter remains finite and meaningful. The thermodynamic limit also preserves the discrete (in space) character of the evolution equations and therefore the corresponding equilibrium states can differ in character from those obtained from a continuum limit. We will discuss some of these differences in the fol-

lowing section where we derive and analyze the dispersion relation for plane waves for our discrete set of equations (1).

III. DISPERSION RELATION FOR PLANE WAVES

We seek plane wave solutions of Eq. (1) of the form

$$\Psi_j = Re^{i(jka+\omega t)}, \tag{3}$$

where a is the distance between any two adjacent oscillators and k is the wave number such that $-\pi \leqslant ka \leqslant \pi$. The values of ka, which define the phase difference between adjoining oscillators, are further constrained by the periodicity conditions inherent in a closed chain configuration. Since ψ_{N+1} must be identical to ψ_1 and ψ_0 must be identical to ψ_N, we must satisfy the condition $e^{iNka}=1$. This implies that $Nka = 2m\pi$, $m=0,1,\ldots,N-1$, that is,

$$ka = m\frac{2\pi}{N}, \quad m = 0,1,\ldots,N-1. \tag{4}$$

These discrete values of ka are one of the defining properties of the various phase-locked states of the coupled set of oscillators. Further characteristics of these states are described by a dispersion relation which can be obtained by substituting Eq. (3) in Eq. (1) to give $i\omega = 1 + i\omega_0 - R^2 + 2K[\cos(ka)e^{-i\omega\tau} - 1]$. This leads to

$$\omega = \omega_0 - 2K\sin(\omega\tau)\cos(ka), \tag{5}$$

$$R^2 = 1 - 2K + 2K\cos(\omega\tau)\cos(ka). \tag{6}$$

Equations (5) and (6) which constitute the dispersion relation for plane waves of our model equations can be compared to the corresponding dispersion relation obtained from the CGLE, where we can substitute $\psi(x,t) = R_{CGL}\exp(ikx - i\omega_{CGL}t)$ in Eq. (2) to get

$$\omega_{CGL} = \omega_0, \tag{7}$$

$$R^2_{CGL} = 1 - K(ka)^2, \tag{8}$$

where we have replaced K by its scaled value. Equations (7) and (8) can also be recovered from Eqs. (5) and (6) by setting $\tau=0$ and taking the long wavelength limit of $ka \ll 1$. As we can see there are significant differences in the two dispersion relations. While Eqs. (5) and (6) are valid for any arbitrary value of N, Eqs. (7) and (8) are strictly valid only in the limit of $N \to \infty$. The spectrum of ka values are therefore continuous for the latter whereas in the former they assume discrete values that are determined by the magnitude of N. For $\tau=0$, Eqs. (5) and (7) become identical, but Eq. (6) reduces to

$$R^2 = 1 - 2K + 2K\cos(ka) = 1 - 4K\sin^2(ka/2). \tag{9}$$

Using $R^2 > 0$ as the defining condition for the possibility of having a phaselocked state, we see that this region is considerably reduced in the case of the CGLE as compared to the discrete model equations for any given value of the coupling parameter K. For example, at $K=1/4$, the discrete model allows all modes from 0 to π to exist, whereas the continuum model has an upper cutoff at $ka=2.0$. For $K>1/4$, cutoff regions also appear for the discrete model and are given by the expression

$$f_1 = \cos^{-1}(1 - 1/2K) < ka < f_2 = 2\pi - \cos^{-1}(1 - 1/2K).$$

As can be seen from the above expression, for $K>1/4$ the anti-phase-locked state ($ka=\pi$) is now no longer a permitted state. With the introduction of time delay, the existence region is not only a function of ka (for a given value of K) but also depends on ω which satisfies the transcendental equation (5). This brings about a significant modification of the existence domains and raises the interesting possibility of enabling many of the previously forbidden modes to exist. Since the dispersion relation now has a transcendental character it also introduces additional branches of collective oscillations. To illustrate some of these modifications we consider a few simple examples. Let $C=\cos(\omega\tau)$. By choosing a value for C and in turn defining $S=\sin(\omega\tau)$, we can immediately get an expression for ω, and the resultant equation for R^2 defines the stability regions.

Case (i). First let $\cos(\omega\tau)=1$. This gives $\omega=\omega_0$, and the square of the amplitude as $A_1 = 1 - 2K + 2K\cos(ka)$. This also leads us to $\tau = 2n\pi/\omega_0$, $n=0,1,2,\ldots$. This case also includes the special case of $\tau=0$. Since $A_1 > 0$ for the existence of the solutions, it is easily seen that the bounding region in (K,ka) plane is defined by

$$f_1 < ka < f_2 = 2\pi - f_1,$$

where $f_1 = \cos^{-1}(1-1/2K)$ is the forbidden region. Since f_1 does not intersect with the K axis at any finite K, the region exists for all $K>1/4$. In particular, the in-phase state exists for all $K>0$, and the anti-phase-locked state ($ka=\pi$) no longer exists if $K>1/4$. This forbidden region is illustrated in Fig. 1(a).

Case (ii). Let $\cos(\omega\tau)=1/2$. This gives the dispersion relation $\omega = \omega_0 - \sqrt{3}\cos(ka)$. The corresponding delays are defined by $\tau = (2n \pm 1/3)\pi/[\omega_0 - \sqrt{3}K\cos(ka)]$, $n=0,1,$

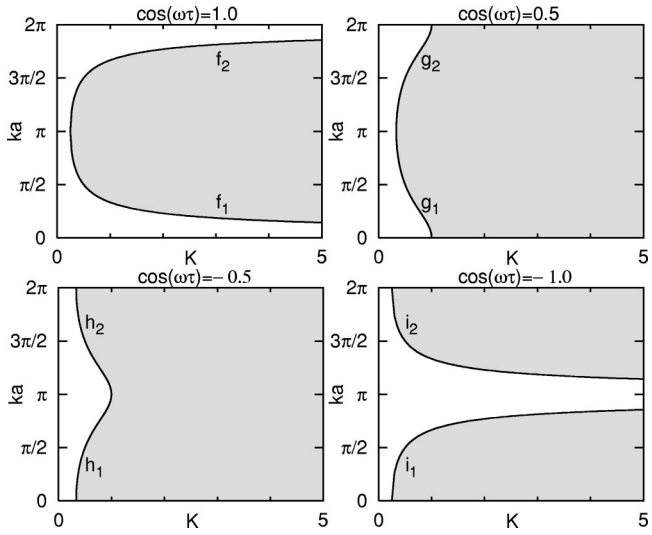

FIG. 1. Allowed (unshaded) and forbidden (shaded) wave modes in the presence of time delay for various values of $\cos(\omega\tau)$.

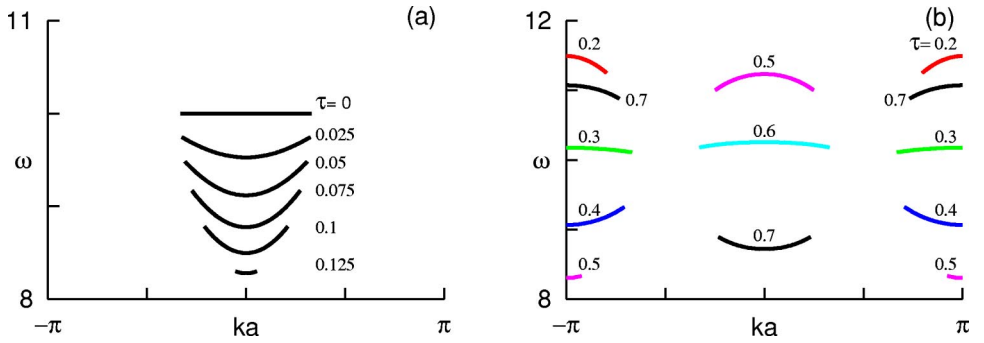

FIG. 2. (Color online) Dispersion relation between allowed wave numbers and the corresponding frequency shown as τ is gradually increased. $K=1$ and $\omega_0=10$. A range of τ values is forbidden.

2,..... The square of the amplitude is given by $A_2=1-2K+K\cos(ka)$. Let $g_1=\cos^{-1}(2-1/K)$. The curve g_1 assumes values for K between $1/3$ and 1. If $K>1$, $A_2<0$ for any ka. So all the modes are forbidden if $K>1$, and the region between $K=1/3$ and $K=1$ as defined by

$$g_1 < ka < g_2 = 2\pi - g_1$$

is also forbidden. In particular the in-phase solutions do not exist if $K>1$ and the antiphase solutions do not exist if $K>1/3$. This region is illustrated in Fig. 1(b).

Case (iii). Let $\cos(\omega\tau)=-1/2$. This gives the dispersion relation $\omega=\omega_0+\sqrt{3}\cos(ka)$. The corresponding delays are defined by $\tau=(2n\pm 1/3)\pi/[\omega_0+\sqrt{3}K\cos(ka)], n=0,1,2,\ldots$. The square of the amplitude is given by $A_3=1-2K-K\cos(ka)$. Let $h_1=\cos^{-1}(1/K-2)$. If $K>1$, $A_3<0$ for all ka. So $K>1$ is the forbidden region. Between $K=1/3$ and $K=1$ the region defined by

$$h_1 > ka > h_2 = 2\pi - h_1$$

is forbidden. The inequality signs are reversed in this case because the curvature of h_1 is different from that of g_1 or f_1. In particular, the in-phase solutions are forbidden if $K>1/3$ and the anti-phase solutions are forbidden if $K>1$. This region is illustrated in Fig. 1(c).

Case (iv). Let $\cos(\omega\tau)=-1$. This results in the dispersion relation $\omega=\omega_0$ just as in case (i). This case corresponds to $\tau=(2n\pi+1)\pi/\omega_0, n=0,1,2,\ldots$. The square of the amplitude is given by $A_4=1-2K-2K\cos(ka)$. Since $A_4=1$ at $ka=\pi$, in contrast to the three previous cases, the anti-phase-locked solutions exist for all values of K. At $ka=0$, $A_4=1-4K$. So the in-phase solutions are forbidden for all $K>1/4$. The forbidden regions when $K>1/4$ are defined by

$$i_1 > ka > i_2 = 2\pi - i_1,$$

where $i_1=\cos^{-1}(1/2K-1)$. This region is illustrated in Fig. 1(d). In fact, we can derive a general expression for the existence curves by choosing any arbitrary value for C. This in turn defines the frequencies as $\omega=\omega_0-2KS\cos(ka)$. After some simple algebra, the corresponding delays are given as

$$\tau=(2n\pi+\cos^{-1}C)/[\omega_0-2KS\cos(ka)] \quad \text{if} \quad S\geqslant 0,$$

$$\tau=(2n\pi-\cos^{-1}C)/[\omega_0-2KS\cos(ka)] \quad \text{if} \quad S<0.$$

The curve that defines the boundary of the forbidden region is given by $j_1=\cos^{-1}(1/S-1/2\,KS)$ when $S\neq 0$. The case of $S=0$ is the same as case (i) studied above.

Apart from these special cases, the general existence regions are complicated functions of ka, K, and τ. They need to be determined numerically by simultaneous solution of Eqs. (5) and (6). To demonstrate the constraint imposed by Eq. (5) we have plotted its solution (ω vs ka) for various values of τ and for a fixed value of ω_0 and K in Fig. 2(a). When $\tau=0$, the allowed range of τ is given by $\text{abs}(ka)<\cos^{-1}(1-1/2K)$. So for $K=1$, the phase-locked patterns that have wave numbers less than $\pi/3$ are allowed, and all of them have an identical frequency. As τ is increased the frequency of oscillation decreases for small τ, and the dispersion relation acquires a nonlinear parabolic character. As τ is further increased, depending on the actual value of K, there are bands in τ values where no modes exist. The shrinking and disappearance of the dispersion curve at $ka=0$ beyond $\tau=0.125$ up to $\tau=0.2$ in Figs. 2(a) and 2(b) illustrate this phenomenon. One also notices from Fig. 2(b) that at higher values of τ the dispersion curves become discontinuous and have bands of forbidden ka regions.

IV. STABILITY OF PHASE-LOCKED SOLUTIONS

We now find the stability of the equilibrium phase-locked solutions discussed in the preceding section by carrying out a linear perturbation analysis. Let

$$\psi_j(t)=[R_k e^{i\omega_k t}+u_j(t)]e^{i(jka)}, \tag{10}$$

where $k=0,1,\ldots,N-1$. Substitution of Eq. (10) in Eq. (1) yields in the lowest order the dispersion relation discussed in the preceding section. In the next order, where we retain terms that are linear in the perturbation amplitude, we observe that

$$|\psi_k|^2\psi_k=\cdots+[2R_k^2u_j(t)+R_k^2e^{2i\omega_k t}\overline{u_j}(t)]e^{i(jka)}+\cdots. \tag{11}$$

Using the above, we obtain the equation

$$\frac{\partial u_j(t)}{\partial t} = (1 + i\omega_0 - 2R_k^2 - 2K)u_j(t) - R_k^2 e^{2i\omega_k t}\overline{u_j}(t) + K[u_{j+1}(t-\tau)e^{ika} + u_{j-1}(t-\tau)e^{-ika}] \quad (12)$$

and, taking its complex conjugate,

$$\frac{\partial \overline{u_j}(t)}{\partial t} = (1 - i\omega_0 - 2R_k^2 - 2K)\overline{u_j}(t) - R_k^2 e^{-2i\omega_k t}u_j(t) + K[\overline{u_{j+1}}(t-\tau)e^{-ika} + \overline{u_{j-1}}(t-\tau)e^{ika}]. \quad (13)$$

Multiply Eqs. (12) and (13) term by term by $e^{i(jqa)}$, make use of the identities

$$u_{j\pm1}(t-\tau)e^{\pm ika}e^{i(jqa)} = u_{j\pm1}(t-\tau)e^{i(j\pm1)qa}e^{\pm i(k-q)a} \quad (14)$$

and

$$\overline{u_{j\pm1}}(t-\tau)e^{\mp ika}e^{i(jqa)} = \overline{u_{j\pm1}}(t-\tau)e^{i(j\pm1)qa}e^{\mp i(k+q)a}, \quad (15)$$

and sum over $j=0,1,2,\ldots,N-1$. Introducing adjoint amplitudes $w_q(t)$ and $\tilde{w}_q(t)$ by the definitions

$$[w_q(t),\tilde{w}_q(t)] = \sum_{j=0}^{N-1}[u_j(t),\overline{u_j}(t)]e^{i(jqa)}, \quad (16)$$

we obtain the set of coupled equations

$$\frac{dw_q(t)}{dt} = (1 + i\omega_0 - 2R_k^2 - 2K)w_q(t) - R_k^2 e^{2i\omega_k t}\tilde{w}_q(t) + 2K\cos[(k-q)a]w_q(t-\tau) \quad (17)$$

and

$$\frac{d\tilde{w}_q(t)}{dt} = (1 - i\omega_0 - 2R_k^2 - 2K)\tilde{w}_q(t) - R_k^2 e^{-2i\omega_k t}w_q(t) + 2K\cos[(k+q)a]\tilde{w}_q(t-\tau). \quad (18)$$

In order to perform the stability analysis, we assume solutions of the form

$$[w_q(t),\tilde{w}_q(t)] = [ce^{i\omega_k t},\tilde{c}e^{-i\omega_k t}]e^{\lambda t}, \quad (19)$$

which yield the set of coupled equations

$$C_+ c + R_k^2\tilde{c} = 0, \quad (20)$$

$$R_k^2 c + C_-\tilde{c} = 0. \quad (21)$$

In these equations, the quantities $C_\pm$ are given by

$$C_\pm = \lambda - [1 \pm i(\omega_0 - \omega_k) - 2R_k^2 - 2K] - 2K\cos[(k \mp q)a]e^{\mp i\omega_k\tau}e^{-\lambda\tau}. \quad (22)$$

The eigenvalue equation is obtained from the determinantal condition for Eqs. (20) and (21), namely,

$$C_+C_- - R_k^4 = 0. \quad (23)$$

This can be expanded to be written in the form of the following characteristic equation:

$$\lambda^2 + (a_1 + a_2)\lambda + (a_1a_2 - R^4) = 0, \quad (24)$$

where $a_1 = 2R^2 - 1 + 2K - i(\omega_0 - \omega) - 2K\cos[(k-q)a]e^{-(\lambda+i\omega)\tau}$, $a_2 = 2R^2 - 1 + 2K + i(\omega_0 - \omega) - 2K\cos[(k+q)a]e^{-(\lambda-i\omega)\tau}$.

It should be noted that the perturbation wave numbers q are once again a discrete set and from the periodicity requirement they obey the relation

$$qa = m\frac{2\pi}{N}, \quad m = 0,1,\ldots,N-1.$$

Thus in our stability analysis any pattern corresponding to a given value of ka, we need to examine the eigenvalues of Eq. (24) at each of the above permitted values of qa. We now proceed to discuss the stability of the various phase-locked patterns both in the absence and presence of time delay.

A. Stability of phase-locked patterns in the absence of delay

In the absence of time delay, the eigenvalue equation (24) can be solved analytically to give

$$\lambda = 1 - 2R^2 - 2K + 2K\cos(ka)\cos(qa) \pm \sqrt{4K^2\sin^2(ka)\sin^2(qa) + R^4}. \quad (25)$$

The real parts of the eigenvalues of Eq. (24) will be negative if $a_1 + a_2 > 0$ and $a_1a_2 - R^4 > 0$ simultaneously. The first of these conditions can be simplified to give

$$a_1 + a_2 = 2[1 - 2K\{1 - \cos(ka)[2 - \cos(qa)]\}] > 0, \quad (26)$$

and the second condition can be simplified to give

$$a_1a_2 - R^4 = [1 - \cos(qa)]4K[K\{4\cos^2(ka) - 2\cos(ka) - [1 + \cos(qa)]\} + \cos(ka)] > 0. \quad (27)$$

In the following, we use these two conditions, or, in the simplest cases, the eigenvalue equation itself to determine the stability.

1. In-phase patterns ($k=0$ mode)

From the preceding section the $k=0$ solution is given by $\omega=\omega_0$ and $R=1$. Substituting these in Eq. (25) above and setting $k=0$ we get

$$\lambda = \begin{cases} -2K[1 - \cos(qa)] \leqslant 0 \\ -2 - 2K[1 - \cos(qa)] < 0. \end{cases}$$

Thus the plane wave solution $\Psi_j(t) = e^{i\omega_0 t}$, which is nothing but an in-phase locked solution of the coupled identical oscillators, is stable for $\tau=0$ for all values of ω_0.

2. Antiphase patterns ($ka=\pi$ mode)

The equilibrium pattern in this case consists of adjacent oscillators remaining π out of phase at all times and oscillating with the same frequency ω_0. The amplitude of the oscillations is given by

$$R^2 = 1 - 4K.$$

As discussed in the preceding section, the condition $R^2 > 0$ permits the existence of this mode in the region of $K < 1/4$. However as we will see below, using conditions (26) and (27), these permitted antiphase states are linearly unstable for any arbitrary number of oscillators. Inserting $ka = \pi$ in Eqs. (26) and (27) the conditions simplify to

$$K < \min \frac{1}{2[3 - \cos(qa)]} \tag{28}$$

and

$$K > \max \frac{1}{5 - \cos(qa)}, \tag{29}$$

where the qa values are to be determined as per the prescription discussed in the preceding section. As simple examples, for $N=2$ the only permitted values of qa are 0 and π and from Eqs. (28) and (29) above, we arrive at the requirement that $K < 1/8$ and $K > 1/4$, which is not possible. Hence the mode is unstable. Such conditions were previously obtained by Aronson *et al.* [16] in their investigation of the collective states of two coupled limit cycle oscillators. In fact, the argument can be extended to any arbitrary even N since

$$5 - \cos(qa) \leqslant 2[3 - \cos(qa)]$$

for all values of qa and hence the conditions (28) and (29) cannot be satisfied simultaneously for any value of K. This implies that the antiphase states, characterized by $ka = \pi$, are unstable for any arbitrary value of even N.

3. Other phase-locked patterns ($k > 0$)

Another interesting phase-locked pattern is the $k = \pi/2$ mode. It can be shown by using the conditions discussed above that this pattern is also always unstable. However, a large number of other modes whose wave numbers are close to either 0 or 2π are likely to be stable. They coexist with the in-phase stable solutions ($ka = 0$). The relations (26) and (27) provide sufficient conditions to find the stability of any given mode. The contours of $a_1 + a_2 = 0$ and $a_1 a_2 - R^4 = 0$ are given, respectively, by

$$qa = \{\cos^{-1}[2 - (2K - 1)/2KC], \; 2\pi - \cos^{-1}[2 - (2K - 1)/2KC]\},$$

$$qa = \{\cos^{-1}[C(1/K - 2 + 4C) - 1], \; 2\pi - \cos^{-1}[C(1/K - 2 + 4C) - 1]\},$$

where $C = \cos(ka)$. These curves are plotted in Fig. 3 for $K = 0.4$. We see that there is a large range of ka values that satisfies the conditions (26) and (27). For a given number N of oscillators if the ka values fall in this range then the corresponding phase-locked patterns are stable. The x-axis intersections of the curve $a_1 a_2 - R^4 = 0$, which are closer to 0 and 2π provide boundaries of K below which the modes are stable. By setting $qa = 0$ in Eq. (27), we obtain the condition on K for stability as a function of ka:

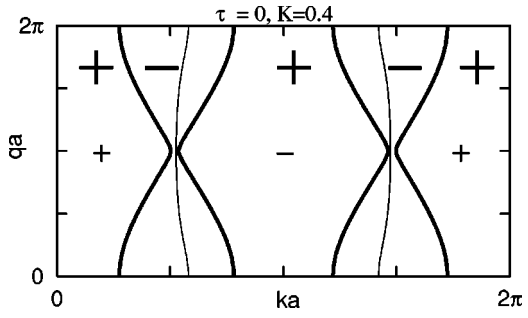

FIG. 3. The contours of $a_1 + a_2 = 0$ (thin lines) and that of $a_1 a_2 - R^4 = 0$ (thick lines). The thin + and − signs indicate the sign of $a_1 + a_2$ in the connected regions bounded by the thin curves, and the thick signs indicate the sign of $a_1 a_2 - R^4$ in those bounded by the thick curves.

$$K < \frac{-\cos(ka)}{2[2\cos^2(ka) - \cos(ka) - 1]} \equiv K^*. \tag{30}$$

This stability region is plotted in Fig. 4. In the limit of $N \to \infty$, a continuous range of ka modes are accessible, and the system truly possesses infinitely many stable phase-locked states when $K < K^*$. The stability of these phase-locked solutions is one important result of our paper. Note that all phase-locked patterns with wave numbers between $\pi/2$ and $3\pi/2$ are unstable. We also note from Fig. 4 that for a given value of K it is possible to have more than one stable state corresponding to different values of ka that lie in the two stable regions. In the limit of $N \to \infty$ such a multistability phenomenon can occur over a continuous range of ka values spanning the stable regions. A numerical example of the multistability of some of these modes is illustrated in Fig. 5 for $N = 50$ oscillators at a fixed value of $K = 0.4$. By giving initial conditions close to the modes $ka = 2\pi/50$, $4\pi/50$, and $6\pi/50$, the corresponding phase-locked solutions are realized.

Now we address the following question. What is the minimum number of oscillators for which a second phase-locked

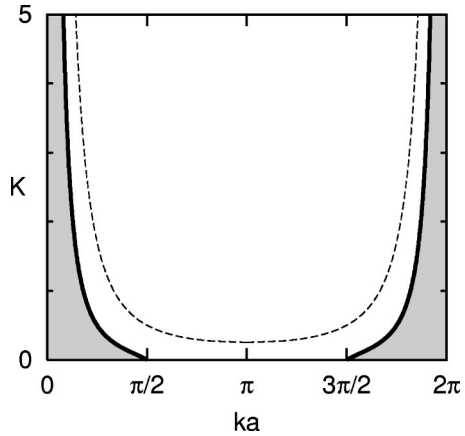

FIG. 4. The stability region of the phase-locked states (shaded region which is below $K = K^*$) plotted in (K, ka) space. The left half of the dashed curve is f_1 and the right half is f_2 as drawn in Fig. 1(a).

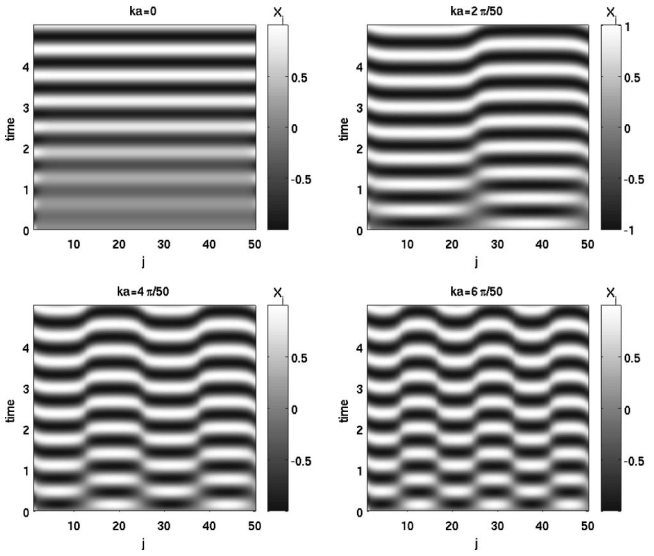

FIG. 5. Multiple stable phase-locked patterns for $N=50$ at $\omega_0=10$ and $K=0.4$ in the absence of time delay. The real parts of the complex vector $Z_j(t)$ are plotted in gray scale.

pattern (the first one being in-phase) can become stable? Since the permissible *ka* values are related to the number of oscillators *N* in an inverse fashion due to the periodicity requirement [see Eq. (4)] we need to determine the maximum stable *ka* in order to find the minimum critical *N*. Since $K=K^*$ makes an intersection at $ka=\pi/2$ and $ka=3\pi/2$, the second stable phase-locked pattern that could emerge at this point will have

$$ka = m\frac{2\pi}{N} = \frac{\pi}{2}.$$

Hence $N \geqslant 4$ for a second phase-locked pattern to ever become stable. Thus for $N=2$ or $N=3$ coupled identical oscillators we will only have in-phase oscillations as stable oscillations and there will not be any other stable phase-locked states. The minimum number of oscillators necessary for multistable behavior is four. Thus $N=4$ is a critical number.

B. Phase-locked patterns for finite time delay

Now we study the synchronized patterns that could become stabilized by the presence of time delay. We noted before that, in the absence of time delay, the in-phase oscillations are always stable, and the antiphase oscillations are always unstable for any positive finite *K*. Time delay changes the scenario and could make each of these branches stable in certain ranges of τ. In addition, the number of multiple branches of each of these two oscillations increases with τ. Equations (5) and (6) define the amplitudes and frequencies of these synchronized states, and the characteristic equation (24) determines their linear stability.

We begin with a simple example of two coupled oscillators, $N=2$, which can have just two phase-locked states, namely, in-phase states with $ka=0$ and antiphase states with $ka=\pi$. We evaluate the eigenvalues for these two cases for different values of τ by numerically solving Eq. (24) for the

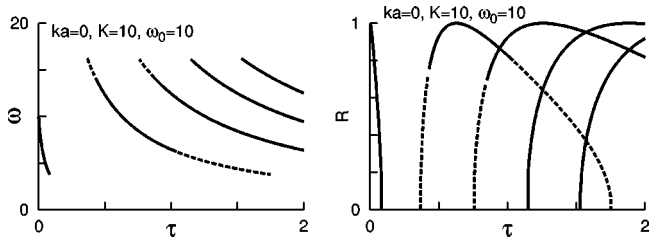

FIG. 6. The in-phase ($ka=0$) locked frequencies and amplitudes represented by Eq. (1) at $K=10$ and $\omega_0=10$. The dashed portions represent the unstable branches for the case of $N=2$ and the continuous lines represent the stable branches.

permitted values of *qa* and also confirm the existence of the modes by an actual integration of the original equations. We show the stable (continuous) and unstable (dashed lines) branches of these two solutions in Figs. 6 and 7. A stable in-phase branch emerges from $\tau=0$ and its amplitude becomes 0 while its frequency is finite showing a supercritical Hopf bifurcation. The first branch of the anti-phase-locked state emerges from zero again in a supercritical Hopf. As τ is increased multiple Hopf bifurcation points are seen. Such stability of the in-phase and antiphase oscillations were earlier studied by us experimentally using coupled electronic oscillators [40].

As a second illustration, we consider the case of $N=10$, $\tau=\pi/\omega_0$ [i.e. $\cos(\omega\tau)=-1.0$], whose equilibrium existence domain we have discussed earlier as case (iv) in Sec. III. In particular we have noted that the $ka=\pi$ state is a permitted equilibrium state. To examine its stability we observe that we need to examine the eigenvalues for $qa=m(2\pi/N)$, $m=0,1,\ldots,N-1$. In Fig. 8 we have plotted the real part of the eigenvalues for all these perturbation wave numbers. We see that they are all negative, which indicates stability of the pattern. In fact, in this case, due to the symmetry of the characteristic equation we can predict stability for all higher values of *N* as well with the eigenvalues of all additional *qa* values falling on the dotted line shown in the figure. The existence regions for this case were shown in Fig. 1(d). By considering this case for all the possible values of *qa* between 0 and 2π, we are essentially determining the stability of this case in the infinite oscillator limit. We show our numerical results for this case in Fig. 9. It is obtained by tracking the eigenvalue transitions for *qa* between 0 and 2π. This phase diagram is strictly true for $N\to\infty$. As can be seen,

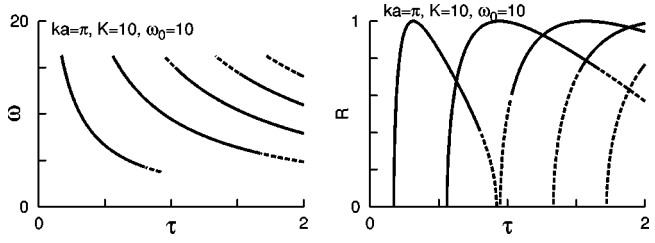

FIG. 7. The antiphase ($ka=\pi$) locked frequencies and amplitudes represented by Eq. (1) at $K=10$ and $\omega_0=10$. The dashed portions represent the unstable branches for the case of $N=2$ and the continuous lines represent the stable branches.

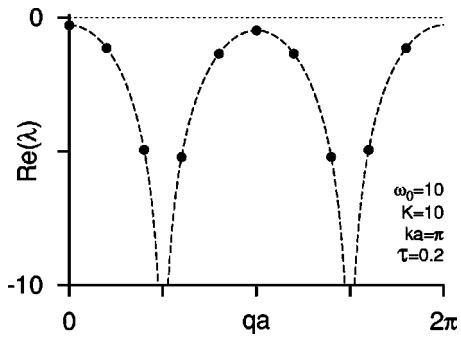

FIG. 8. Real part of the eigenvalues as a function of qa for $N=10$ at $\omega_0=10$, $K=10$, $ka=\pi$, and $\tau=0.2$.

finite τ increases the number of stable modes for any given value of K. We finally show in Fig. 10 a numerical example of the anti-phase oscillations using $N=50$ oscillators.

V. AMPLITUDE DEATH FOR FINITE TIME DELAY

As is well known, a system of identical oscillators that are globally coupled do not have an amplitude death state [16] but the presence of time delay in the coupling can bring about such a collective state. This phenomenon was first pointed out for two coupled oscillators in [35] and also generalized to N globally coupled oscillators [36]. A similar statement also holds for locally coupled oscillators as will be shown. The death state in the presence of time delay had earlier been numerically confirmed for a finite number of locally coupled oscillators [35]. However, no systematic study of the dependence of the death island regions on the magnitude of the time delay and the number of oscillators has so far been carried out for systems of locally coupled oscillators. In this section we address this issue and study the stability of the origin for our discrete model equation (1). Amplitude death state is characterized by $R=0$. To derive an appropriate set of eigenvalue equations for determining the stability of this state, we carry out a linear perturbation analysis about the origin. Substituting $(\psi_j=0+\tilde{\psi}_j)$ in Eq. (1) and discarding the nonlinearities we get

$$\frac{\partial \tilde{\psi}_j}{\partial t} = (1+i\omega_0)\tilde{\psi}_j + K[\tilde{\psi}_{j+1}(t-\tau) - \tilde{\psi}_j(t)] + K[\tilde{\psi}_{j-1}(t-\tau) - \tilde{\psi}_j(t)], \tag{31}$$

where $j=1,\ldots,N$ with periodic boundary conditions. By letting $\tilde{\psi}(t)\propto e^{i\lambda t}$, the eigenvalue matrix in circulant form is obtained. The determinant of this matrix is written as

$$\prod_{j=1}^{N} (\lambda + 2K - 1 - i\omega_0 - Ke^{-\lambda\tau}U_j - Ke^{-\lambda\tau}U_j^{N-1}) = 0,$$

where $U_j=e^{i2\pi(j-1)/N}$ are the Nth roots of unity. But $U_j+U_j^{N-1}=U_j+U_j^{-1}=2\cos[(j-1)2\pi/N]$. So the above equation takes the form of

$$\prod_{j=1}^{N} (\lambda + 2K - 1 - i\omega_0 - 2K\cos[(j-1)2\pi/N]e^{-\lambda\tau}) = 0. \tag{32}$$

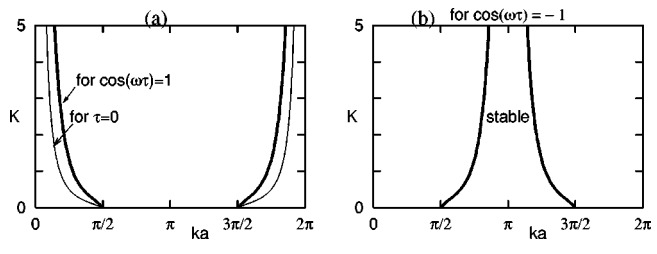

FIG. 9. (a) Critical boundaries below on which stable phase-locked patterns exist are shown for the case of $\cos(\omega\tau)=1$ as $N\to\infty$. (b) Stability region of phase-locked patterns for $\cos(\omega\tau)=-1$ as $N\to\infty$.

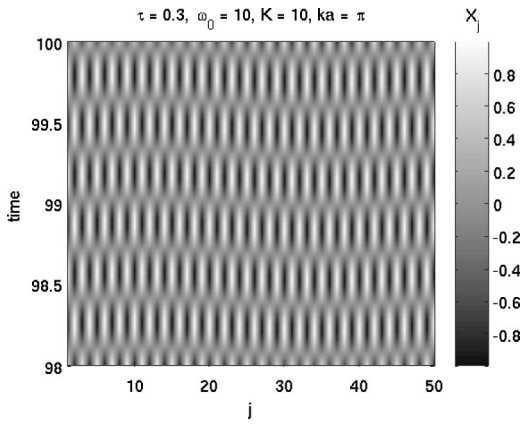

FIG. 10. Anti-phase-locked state of identical oscillators for $N=50$ at $K=10$ and $\tau=0.3$.

The complete set of eigenvalue equations includes the second set obtained by considering the conjugate equation of the above. Note that for $\tau=0$ the above eigenvalue equation (32) always admits at least one unstable eigenvalue, namely $\lambda=1+i\omega_0$. Hence identical oscillators that are locally coupled cannot have an amplitude death state in the absence of time delay. We will now determine the amplitude death regions for finite values of τ. We define a factor $R_j=2\cos[(j-1)2\pi/N]$ that we will use in the critical curves derived below. If the number of oscillators is a multiple of 4, there are some eigenvalue equations that emerge without a dependence on τ, when $R_j=0$. For example, consider the case of $N=4$ and $j=2,4$. Then, the eigenvalue equation becomes $\lambda=1-2K\pm i\omega_0$. For this equation, the only criticality is given by $K=1/2$. The stable region lies on the side of the parameter space that obeys $K>1/2$. For other values of R_j, the death island boundaries can be derived by setting the real part of the eigenvalue to zero, and appropriately choosing the signs of the multiple curves that result. The analysis is similar to the one we presented in the treatment of globally coupled oscillators [35,36], and here we simply provide the final expressions for the critical curves in (τ,K) plane:

$$\tau_a(n,K)=\begin{cases}\dfrac{2n\pi-\cos^{-1}[(2K-1)/KR_j]}{\omega_0+\sqrt{K^2R_j^2-(2K-1)^2}}, & R_j>0,\\ \dfrac{(2n+1)\pi-\cos^{-1}[(2K-1)/K|R_j|]}{\omega_0+\sqrt{K^2R_j^2-(2K-1)^2}}, & R_j<0,\end{cases} \tag{33}$$

$$\tau_b(m,K)=\begin{cases}\dfrac{2m\pi+\cos^{-1}[(2K-1)/KR_j]}{\omega_0-\sqrt{K^2R_j^2-(2K-1)^2}}, & R_j>0,\\ \dfrac{(2m+1)\pi+\cos^{-1}[(2K-1)/K|R_j|]}{\omega_0-\sqrt{K^2R_j^2-(2K-1)^2}}, & R_j<0.\end{cases} \tag{34}$$

n and m are whole numbers. We now determine some useful bounds on K for ordering and finding the degeneracies of the critical curves. The argument of inverse cosine functions and the square root term in the denominators of the above expressions impose the following bounds on K:

$$K>1/4 \quad \text{for} \quad R_{j=1}, \tag{35}$$

$$\frac{1}{2+R_j}<K<\frac{1}{2-R_j} \quad \text{for} \quad R_{j>1}. \tag{36}$$

The sign of the derivative with respect to τ of the real part of the eigenvalue is determined by the term $-\mathrm{Im}(\lambda)KR_j\sin[\mathrm{Im}(\lambda)\tau]$, and after some algebra it is expressed as

$$\left.\frac{d\mathrm{Re}(\lambda)}{d\tau}\right|_{\mathrm{Re}(\lambda)=0} \begin{cases}>0, & \text{on } \tau_a, \quad \text{for any } \omega_0\\ <0, & \text{on } \tau_b, \quad \text{if} \quad \omega_0>\sqrt{K^2R_j^2-(2K-1)^2}\\ >0, & \text{on } \tau_b, \quad \text{if} \quad \omega_0<\sqrt{K^2R_j^2-(2K-1)^2}.\end{cases} \tag{37}$$

The first condition involving ω_0 in the above relation leads to the following bounds on K:

$$K<(1+\omega_0^2)/4, \quad \text{for} \quad R_{j=1}, \tag{38}$$

$$K>\frac{2+R_j\sqrt{1+\omega_0^2}}{4-R_j^2} \quad \text{or} \quad K<\frac{2-R_j\sqrt{1+\omega_0^2}}{4-R_j^2}, \quad \text{for} \quad R_{j>1}. \tag{39}$$

The ranges of K imposed by the relations (35) and (39) are mutually exclusive. Hence, on the curve τ_b the only boundary across which an eigenvalue pair makes a transition to the negative eigenvalue plane occurs when $R_{j=1}$, and across the curves occurring when $R_{j>1}$, the eigenvalue pair makes a transition to the positive plane. So $\tau_b(0,K)$ at $R_{j=1}$ always remains as the left hand side boundary of the death island. In order to see the degeneracy among the curves, note that

$$R_k=R_j \quad \text{if} \quad k=N+2-j.$$

Also the sign of R_j does not play a role in distinguishing the critical curves. These two properties are responsible for a reduction of the number of the actual distinct boundaries of the death islands. These degeneracies can be framed into two cases. First, when N is odd. The total number of distinct values of R_j is $(N+1)/2$. $R_1(=2)$ is the maximum of all the R_j and is nondegenerate; and R_i, where $i=2,\ldots,(N+1)/2$ are the other distinct values, whose values are identically equal to R_k, where $k=N+2-i$. Among the latter R_j values, the maximum negative value occurs at $j=(N+1)/2$. The curves corresponding to $R_j>0$ and $R_j<0$ form the boundaries for two different death islands, as can be seen from the indices in Eqs. (33) and (34). A further ordering of the curves must be done by a numerical plotting of the curves. The ordering reveals that for $N\leqslant 13$, the first death island is bounded by the curves

$$\gamma_1: \quad \tau_b(0,K) \quad \text{at} \quad R_{j=1},$$

$$\gamma_2: \quad \tau_b(0,K) \quad \text{at} \quad R_{j=(N+1)/2},$$

and

$$\delta_1: \quad \tau_a(0,K) \quad \text{at} \quad R_{j=(N+1)/2},$$

$$\delta_2: \quad \tau_a(1,K) \quad \text{at} \quad R_{j=1}.$$

The curves γ_1 and δ_2 form, respectively, the left and the right boundaries of the death island region. And δ_1 and δ_2 form the bottom two curves. The existence range along K of δ_1, across which the eigenvalues make a transition to the left half plane, increases with increasing N. In fact it intersects with γ_1. So this provides the first boundary across which stability is lost. This occurs for $N\geqslant 15$, when the death island is bounded by the two curves:

$$\gamma_1: \quad \tau_b(0,K) \quad \text{at} \quad R_{j=1}$$

and

$$\delta_1: \quad \tau_a(0,K) \quad \text{at} \quad R_{j=(N+1)/2}.$$

Second, when N is even, many more curves become degenerate. The number of distinct value of R_j is $N/2+1$. Among these distinct values, the magnitudes of pairs of them can become identical. If N is divisible by 4, such pairs are $N/4+1$ in number, and $(N+2)/4$ otherwise. Every positive R_j has its negative counterpart. The maximum value of $R_j=2$ occurs when $j=1$, and the next maximum value is at $R_{j=2}$. Hence Eqs. (33) and (34) can be simplified to

$$\tau_c(n,K)=\frac{n\pi-\cos^{-1}[(2K-1)/KR_j]}{\omega_0+\sqrt{K^2R_j^2-(2K-1)^2}}, \quad R_{j=1,\ldots,J}, \tag{40}$$

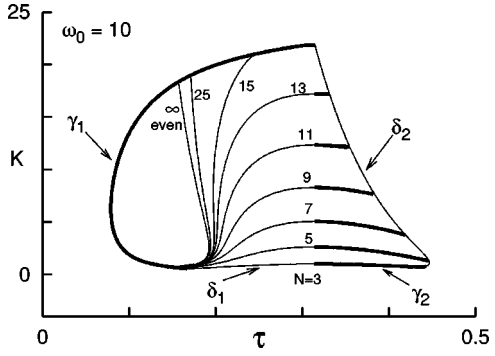

FIG. 11. Death islands at $\omega_0=10$. All even number of oscillators have a single death island region that is independent of the number of oscillators. The odd number of oscillators are bounded by four curves when $N \leqslant 13$, and two curves otherwise. These two curves merge in the infinite limit with the curves that represent the even number of oscillators.

$$\tau_d(m,K) = \frac{m\pi + \cos^{-1}[(2K-1)/KR_j]}{\omega_0 - \sqrt{K^2R_j^2 - (2K-1)^2}}, \quad R_{j=1,\ldots,J}, \quad (41)$$

where $J=N/4+1$ if N is divisible by 4, and $(N+2)/4$ otherwise. The actual ordering, however, reveals that the death island boundaries are given by $\tau_c(0,K)$ at $R_{j=1}$ and $\tau_d(1,K)$ at $R_{j=1}$, which are identical, respectively, to δ_1 and γ_1. These curves are plotted in Fig. 11. As is seen for N even there is a single death region. In the case of N odd the boundary of the death region depends on the value of N. As N increases, the area of the death region decreases. As $N \to \infty$ the area of the death island for N odd decreases and approaches, as a limit, the boundary for N even. For all N, the intersections of γ_1 and δ_1 or those of γ_2 and δ_2 occur for $K>1/2$. So the delay-independent eigenvalue equations that are mentioned earlier do not contribute to the death island boundaries. The differences in the death island boundaries for even and odd numbered oscillators can be traced primarily to the behavior of the eigenvalues of the lowest permitted perturbation wave numbers. For an even number N of oscillators the smallest perturbation mode is $qa=\pi$. The values of the real parts of the eigenvalues corresponding to this mode are close in their magnitude to those corresponding to the $qa=0$ perturbation mode. Across the right hand side boundary of the death island region, the $qa=\pi$ mode grows positive and the system emerges out of the death region with an antiphase state. When N is odd, however, the smallest perturbation mode is $qa=\pi-\pi/N$ which is more heavily damped than the $qa=0$ mode. So the death region continues to exist for larger τ values. Ultimately, the second eigenvalue branch of the $qa=0$ mode (which exists due to the transcendental nature of the eigenvalue equation) grows and the system emerges across the boundary with an in-phase state of a different frequency. As N becomes large, the smallest perturbation mode for the N odd case gets closer to π and the death island boundaries of the two cases, as seen in Fig. 11, become indistinguishable. We have independently verified the death regions depicted in Fig. 11, including their interesting dependence on N, by a direct numerical solution of Eq. (1) over the specified range of parameters. We also illustrate in Fig. 12 an example of the amplitude death state for a chain of $N=50$ oscillators.

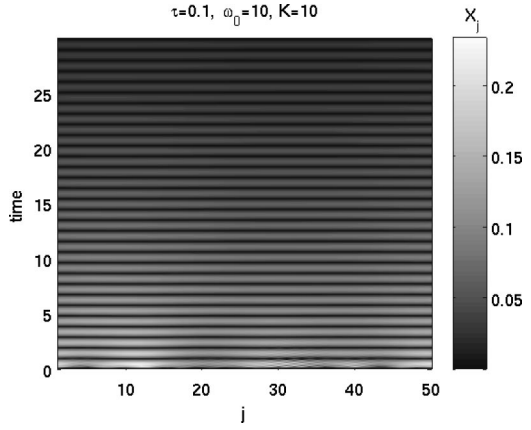

FIG. 12. Amplitude death of identical oscillators for $N=50$ at $K=10$ and $\tau=0.1$.

VI. DISCUSSION AND CONCLUSIONS

We have studied the existence and stability of phase-locked patterns and amplitude death states in a closed chain of delay coupled identical limit cycle oscillators that are near a supercritical Hopf bifurcation. The coupling is limited to nearest neighbors and is linear. The coupled oscillators are modeled by a set of discrete dynamical equations. Using the method of plane waves we have analyzed these equations and obtained a general dispersion relation to delineate the existence regions of equilibrium phase-locked patterns. We have also studied the stability of these states by carrying out a linear perturbation analysis around their equilibria. Our principal results are in the form of analytic expressions that are valid for an arbitrary number of oscillators N (including the $N \to \infty$ thermodynamic limit) and that can be used in a convenient fashion to identify and or obtain stable equilibrium states for a given set of parametric values of time delay, coupling constant, wave number, and wave frequency. We have carried out such an exercise for a number of illustrative cases both with and without the presence of time delay. In the absence of time delay, our analysis reveals a number of new phase-locked states close to the in-phase stable state which can exist simultaneously with the in-phase state. The minimum number of oscillators for which this multirhythmic phenomena can occur is $N=4$. Time delay introduces interesting features in the equilibrium and stability scenario. In general, we have found that time delay expands the range of possible phase-locked patterns and also extends the stability region relative to the case of no time delay. The dispersion curves for varying values of time delay also display some novel features such as forbidden regions and jumps in the range of allowed wave numbers as well as forbidden bands in the space of time delay.

We have also carried out a detailed analytic and numerical investigation of the existence of stable amplitude death states in the closed chain of delay coupled identical limit cycle

oscillators. The results not only confirm our earlier numerical demonstration of the existence of such death states but go beyond to provide a comprehensive picture of the existence regions in the parameter space of time delay and coupling strength. The analytic results also establish that death island regions exist for any number of oscillators N for appropriate vales of K, ω, and τ. In this sense our work provides a generalization of the earlier amplitude death related results, that were obtained for globally coupled oscillators to the case of locally coupled oscillators. An interesting result, arising from the local coupling configuration, is that the size of a *death island* is independent of N when N is even but is a decreasing function of N when N is odd. In other words the death island results for the $N=2$ island hold good for any arbitrary even number of locally coupled oscillators and constitute the minimum size of the death island in the $K-\tau$ parameter space. This can have interesting practical implications. For example, in coupled magnetron or laser applications if one is seeking to minimize the parametric region where death may occur (and thereby greatly diminish the total power output of the system) it is best to select a configuration with an even number of devices. At a more fundamental level this "invariance" property which is strongly dependent on the symmetry of the system may also have interesting dynamical consequences, e.g., in the manner of the collective relaxation toward the death state from arbitrary initial conditions. In fact, we see some evidence of this differing dynamics in our numerical investigations of the time evolution of the system toward the death state. For an even number of oscillators we observe a rapid clustering of the oscillators into two distinct groups that are π out of phase. These two giant clusters then slowly pull each other off their orbits and spiral toward the origin. For an odd number of oscillators the lack of symmetry appears to prevent this grouping, the phase distribution of the oscillators has a greater spread in its distribution, and the relaxation dynamics is distinctly different. As the number of oscillators increases and the asymmetry gets reduced the difference in the dynamical behavior becomes less distinct. In the limit of $N \rightarrow \infty$, the difference vanishes and the size and shape of the odd N island asymptotes to the N-even island. A fundamental understanding of this dynamical behavior and its relation to the symmetry dependence emerging from the stability analysis could be an interesting area of future exploration. Our results could also be useful in applications where locally coupled configurations are employed such as in coupled magnetron devices, coupled laser systems, and neural networks as a roadmap for accessing their various collective states.

[1] S. H. Strogatz, Physica D **143**, 120 (2000), and references therein.
[2] Willis E. Lamb, Jr., Phys. Rev. **134**, A1429 (1964).
[3] P. M. Varangis, A. Gavrielides, T. Erneux, V. Kovanis, and L. F. Lester, Phys. Rev. Lett. **78**, 2353 (1997).
[4] J. Benford, H. Sze, W. Woo, R. R. Smith, and B. Harteneck, Phys. Rev. Lett. **62**, 969 (1989).
[5] P. Hadley, M. R. Beasley, and K. Wiesenfeld, Appl. Phys. Lett. **52**, 1619, (1988).
[6] Michael F. Crowley and Irving R. Epstein, J. Phys. Chem. **93**, 2496 (1989).
[7] Y. Kuramoto, *Chemical Oscillations, Waves, and Turbulence* (Springer, Berlin, 1984).
[8] A. A. Brailove and P. S. Linsay, Int. J. Bifurcation Chaos Appl. Sci. Eng. **6**, 1211 (1996).
[9] A. T. Winfree, *The Geometry of Biological Time* (Springer-Verlag, New York, 1980).
[10] Atsuko Takamatsu, Reiko Tanaka, Hiroyasu Yamada, Toshiyuki Nakagaki, Teruo Fujii, and Isao Endo, Phys. Rev. Lett. **87**, 078102 (2001).
[11] J. J. Collins and Ian Stewart, Biol. Cybern. **71**, 95 (1994).
[12] M. C. Cross and P. C. Hohenberg, Rev. Mod. Phys. **65**, 851 (1993).
[13] Y. Kuramoto, Prog. Theor. Phys. **56**, 724 (1976).
[14] Y. Kuramoto and I. Nishikawa, J. Stat. Phys. **49**, 569 (1987).
[15] K. Bar-Eli, Physica D **14**, 242 (1985).
[16] D. G. Aronson, G. B. Ermentrout, and N. Kopell, Physica D **41**, 403 (1990).
[17] G. B. Ermentrout, Physica D **41**, 219 (1990).
[18] P. C. Matthews and S. H. Strogatz, Phys. Rev. Lett. **65**, 1701 (1990).
[19] P. C. Matthews, R. E. Mirollo, and S. H. Strogatz, Physica D **52**, 293 (1991).
[20] R. A. Oliva and S. H. Strogatz, Int. J. Bifurcation Chaos Appl. Sci. Eng. **11**, 2359 (2001).
[21] E. I. Volkov and D. V. Volkov, Phys. Rev. E **65**, 046232 (2002).
[22] G. B. Ermentrout and N. Kopell, SIAM (Soc. Ind. Appl. Math.) J. Appl. Math. **50**, 1014 (1990).
[23] L. W. Ren and B. Ermentrout, Physica D **143**, 56 (2000).
[24] S. H. Strogatz, R. E. Mirollo, and P. C. Matthews, Phys. Rev. Lett. **68**, 2730 (1992).
[25] E. Niebur, H. G. Schuster, and D. M. Kammen, Phys. Rev. Lett. **67**, 2753 (1991).
[26] Y. Nakamura, F. Tominaga, and T. Munakata, Phys. Rev. E **49**, 4849 (1994).
[27] Seunghwan Kim, Seon Hee Park, and C. S. Ryu, Phys. Rev. Lett. **79**, 2911 (1997).
[28] S. R. Campbell and D. Wang, Physica D **111**, 151 (1998).
[29] Eugene M. Izhikevich, Phys. Rev. E **58**, 905 (1998).
[30] G. B. Ermentrout and N. Kopell, Proc. Natl. Acad. Sci. U.S.A. **95**, 1259 (1998).
[31] M. K. S. Yeung and S. H. Strogatz, Phys. Rev. Lett. **82**, 648 (1999).
[32] P. C. Bressloff and S. Combes, Physica D **130**, 232 (1999).
[33] P. C. Bressloff and S. Combes, Physica D **126**, 99 (1999).
[34] Matthew G. Earl and Steven H. Strogatz, Phys. Rev. E **67**, 036204 (2003).
[35] D. V. Ramana Reddy, A. Sen, and G. L. Johnston, Phys. Rev. Lett. **80**, 5109 (1998).

[36] D. V. Ramana Reddy, A. Sen, and G. L. Johnston, Physica D **129**, 15 (1999).
[37] Fatihcan M. Atay, Physica D **183**, 1 (2003).
[38] Fatihcan M. Atay, Phys. Rev. Lett. **91**, 094101 (2003).
[39] R. Herrero, M. Figueras, R. Rius, F. Pi, and G. Orriols, Phys. Rev. Lett. **84**, 5312 (2000).
[40] D. V. Ramana Reddy, A. Sen, and G. L. Johnston, Phys. Rev. Lett. **85**, 3381 (2000).
[41] A. Takamatsu, T. Fujii, and I. Endo, Phys. Rev. Lett. **85**, 2026 (2000).
[42] S. H. Strogatz, Nature (London) **410**, 268 (2001), and references therein.
[43] P. C. Bressloff, S. Coombes, and B. de Souza, Phys. Rev. Lett. **79**, 2791 (1997).
[44] Martin Golubitsky and Ian Stewart, *Multiparameter Bifurcation Theory*, Contemporary Mathematics, Vol. 56 (American Mathematical Society, Providence, RI, 1986), pp. 131–173.
[45] José María Fullana, Patrice Le Gal, Maurice Rossi, and Stéphane Zaleski, Physica D **102**, 37 (1997).
[46] Raúl Montagne and Pere Colet, Phys. Rev. E **56**, 4017 (1997).
[47] J. F. Ravoux, S. Le Dizès, and P. Le Gal, Phys. Rev. E **61**, 390 (2000).